

Neural networks for harmonic structure in music perception and action

Bianco R.¹, Novembre G.², Keller, P.E.², Kim SG¹, Scharf, F.¹, Friederici A.D.¹, Villringer A.¹, Sammler D.¹

¹ Max Planck Institute for Human Cognitive and Brain Sciences, Leipzig, Germany

² The MARCS Institute for Brain, Behaviour and Development, Western Sydney University, Sydney, Australia

Address correspondence to:

Roberta Bianco,

Max Planck Institute for Human Cognitive and Brain Sciences

Stephanstr. 1a, 04103 Leipzig, Germany

phone: +49 341 9940 2640

Email: bianco@cbs.mpg.de

1 **Abstract**

2 The ability to predict upcoming structured events based on long-term knowledge and
3 contextual priors is a fundamental principle of human cognition. Tonal music triggers
4 predictive processes based on structural properties of harmony, i.e., regularities defining the
5 arrangement of chords into well-formed musical sequences. While the neural architecture of
6 structure-based predictions during music *perception* is well described, little is known about
7 the neural networks for analogous predictions in musical *actions* and how they relate to
8 auditory perception. To fill this gap, expert pianists were presented with harmonically
9 congruent or incongruent chord progressions, either as musical actions (photos of a hand
10 playing chords) that they were required to watch and imitate without sound, or in an auditory
11 format that they listened to without playing. By combining task-based functional magnetic
12 resonance imaging (fMRI) with functional connectivity at rest, we identified distinct sub-
13 regions in right inferior frontal gyrus (rIFG) interconnected with parietal and temporal areas
14 for processing action and audio sequences, respectively. We argue that the differential
15 contribution of parietal and temporal areas is tied to motoric and auditory long-term
16 representations of harmonic regularities that dynamically interact with computations in rIFG.
17 Parsing of the structural dependencies in rIFG is co-determined by both stimulus- or task-
18 demands. In line with contemporary models of prefrontal cortex organization and dual stream
19 models of visual-spatial and auditory processing, we show that the processing of musical
20 harmony is a network capacity with dissociated dorsal and ventral motor and auditory
21 circuits, which both provide the infrastructure for predictive mechanisms optimising action
22 and perception performance.

23 **Keywords:** Music, harmony, syntax, IFG, functional connectivity, prediction.

24

25 1. Introduction

26 The brain shows a fine sensitivity to patterns and regularities that afford the prediction
27 of incoming events in different domains (Tenenbaum et al., 2011). The theory of predictive
28 coding (Friston, 2010) constitutes a unifying framework for human cognition and considers
29 the brain as a “hypothesis tester” with the goal to optimise perception and action by
30 constantly matching incoming sensory inputs with top-down predictions. Within a multi-level
31 cascade of neural processes at different time scales, higher-level predictions act as priors for
32 lower-level processes based on contextual information, previous exposure and acquired long-
33 term knowledge. Recently, predictive coding theory has been used to explain predictions in
34 the action domain (Kilner et al., 2007), as well as in music perception based on priors related
35 to melodic (pitch) content (Pearce et al., 2010), metric structure (Vuust and Witek, 2014), or
36 harmony (Rohrmeier and Koelsch, 2012). The present study takes a comparative stance on
37 predictions in both music perception and action, with a specific focus on Western tonal
38 harmony.

39 Theoretical accounts refer to harmony as combinatorial arrangement of chords within
40 musical sequences characterized by local and non-local dependencies (Swain, 1995). An
41 instance of these dependencies is that a typical chord progression in Western tonal harmony
42 starts and ends with a reference chord to which some chords are overwhelmingly likely to
43 move to, while they rarely move to others (Tymoczko, 2003). Psychologically, these
44 dependencies are predicted and perceived as tension-resolution patterns by listeners who have
45 been sufficiently exposed to the prevailing musical system (Krumhansl, 1983; Lerdahl and
46 Jackendoff, 1983). Convention in the field of music cognition has that the harmonic
47 principles that govern musical structure are considered as part of a musical “syntax”
48 (Bharucha and Krumhansl, 1983; Koelsch and Siebel, 2005; Patel, 2003), that also includes
49 melodic and/or rhythmic principles of music (Large and Palmer, 2002; Rohrmeier and
50 Koelsch, 2012). Here, we consider “syntax” generally as the knowledge of regularities that
51 control the integration of smaller units into larger musical phrases (Swain, 1995) and thereby
52 support predictions. It is well established that tacit knowledge about structural regularities of
53 music 1) is acquired implicitly (Loui et al., 2009; Rohrmeier and Rebuschat, 2012; Tillmann
54 et al., 2000), 2) largely shapes our musical competence across different musical systems and
55 cultures (Eerola et al., 2006; Lartillot and Ayari, 2011), and 3) enables listeners to cognitively
56 link current auditory items to past events and to generate predictions on forthcoming events
57 (Patel, 2003; Tillmann, 2012). In the present study we will focus on harmonic regularities and
58 investigate how they govern predictions during (auditory) music perception and (silent)
59 musical actions.

60 Harmony not only defines the sequence of musical *sounds* but also co-determines the
61 associated chain of musical *actions*. Therefore, the implicit knowledge of harmonic
62 regularities might influence not only *listeners’* predictions, but also musicians’ *action*
63 planning during performance (Palmer and van de Sande, 1995). While regularity-based

64 predictions during music *listening* have already been thoroughly investigated (Rohrmeier and
65 Koelsch, 2012; Tillmann, 2012), the neural basis of motor predictions in musical *actions* has
66 not been explored in depth (Maidhof et al., 2009; Ruiz et al., 2009). Recent behavioural
67 (Novembre and Keller, 2011) and electrophysiological studies on music production (Bianco
68 et al., 2016; Sammler et al., 2013b) revealed slower response times, higher number of errors
69 and neural processing costs (a centro-parietal negativity) in expert pianists when asked to
70 silently execute harmonically incongruent compared to congruent chord progressions. These
71 costs were associated with the motor reprogramming of a pre-planned, congruent, action in
72 face of an unexpected incongruity, and were taken as indirect evidence that pianists' action
73 planning was based on musical context and internalised knowledge of harmony. In other
74 words, these findings imply that harmonic structure might implicitly regulate mechanisms of
75 motor control to improve music performance beyond fine movement optimization (Bianco et
76 al., 2016; Novembre and Keller, 2011).

77 The goal of the present study is to identify the brain areas involved in motor planning
78 based on the regularities of Western tonal harmony, to explore the connectivity between these
79 areas and to compare this network with the neural network sub-serving analogous processes
80 in auditory music perception. The rationale behind this study is that expert pianists have
81 internalized the rules of harmony not only auditorily but also in the hand action domain. Their
82 substantial motor training should enable them to parse harmonic dependencies also in
83 sequences of silent musical actions to facilitate prediction and planning of forthcoming motor
84 acts during performance. This is because the same harmonic structure in sequences of sounds
85 or sequences of actions without sound (i.e. those movements typically employed for
86 producing these sounds) should trigger cognitive processes that are analogous with regard to
87 the structural information. At the same time, processing should differ between perception and
88 action with regard to the associated sensory and memory retrieval processes (i.e., auditory
89 sound vs. motoric act). Here, we sought to isolate and compare the neural networks involved
90 in harmony processing during either perception or (silent) actions, i.e. to probe the potential
91 contribution of auditory and motor prediction of harmony that are otherwise co-occurring
92 during real music production.

93 Neural hypotheses for musical syntax processing (i.e., harmony) in music *perception*
94 (Koelsch, 2011; Patel, 2003; Tillmann, 2012) posited a special role of frontal computational
95 regions that successively integrate incoming information into higher-order structures by
96 drawing on knowledge about regularities stored in posterior brain regions. Neuroimaging
97 research points to the inferior frontal gyrus (IFG) as the critical computational area that,
98 together with a repository of regularities in posterior auditory regions superior temporal gyrus
99 (STG), affords the prediction of future musical sounds based on the context and listener's
100 long-term music structural knowledge (Kim et al., 2011; Koelsch et al., 2005; Maess et al.,
101 2001; Musso et al., 2015; Sammler et al., 2011; Tillmann et al., 2006). Interestingly, IFG has
102 been associated not only with structural integration and prediction of musical sequences, but

103 also with structuring of complex *actions* (Fuster, 2001; Koechlin and Summerfield, 2007)
104 outside the music domain. Lesions of the left IFG cause impairment in sequencing pictures
105 representing human actions (Fazio et al., 2009), and bilateral IFG are involved in evaluating
106 whether constituent acts belong to the same or separate sub-goals (Farag et al., 2010).
107 Moreover, bilateral IFG activations have been reported during execution of series of motor
108 acts that were organised according to hierarchical action plans (Koechlin and Jubault, 2006).
109 In sum, IFG has become central to hypotheses on processing of structured sequential
110 information in perception and action (Fitch & Martins, 2014; Fiebach & Schubotz, 2006, for
111 various perspectives see Cortex, 2006, vol.2, issue 42), making it conceivable that IFG is also
112 involved in parsing and predicting structural information embedded in musical actions.

113 What has received less attention than the role of IFG, however, is its interaction with
114 task-relevant posterior systems of knowledge during structural processing. In other words,
115 apart from frequently reported co-activations of IFG and auditory temporal regions during
116 music listening (Koelsch and Siebel, 2005), the characterization of other ‘modality-specific
117 regions’, e.g., in musical action, and particularly their connectivity with frontal
118 ‘computational regions’ remains uncertain. In this study, we tested whether pianists’ action
119 planning based on knowledge of Western tonal harmony involves (i) IFG in interaction with
120 (ii) posterior visual-motor areas. Furthermore, we (iii) compared the functional connectivity
121 profiles of IFG during the processing of musical actions and auditory sequences that
122 contained similar harmonic violations.

123 We acquired resting state fMRI data from expert pianists, and then fMRI data during
124 an audio and an action task in which the same harmonic sequences were either auditorily
125 presented or had to be motorically imitated. In the audio task, pianists listened to 5-chord
126 sequences (similar to Koelsch et al., 2005) in which the last chord was either harmonically
127 congruent or incongruent with the preceding musical context. In the action task, in total
128 absence of musical sound, participants were presented with series of photos of a pianist’s
129 hand performing the same congruent/incongruent chord progressions on a piano (Bianco et
130 al., 2016). To engage the motor system in the processing of musical actions, pianists had not
131 only to watch the movements, but also to manually reproduce them on a glass-board. The
132 contrasts of incongruent minus congruent chords during listening or imitation were used to
133 functionally segregate modality-specific areas and to isolate frontal computational areas. To
134 demonstrate crosstalk between these regions, we used the latter as seeds in a functional
135 connectivity analysis of the resting state fMRI data.

136 If harmonic violations of audio sequences activate IFG, then violations of action
137 sequences with the same musical structure should also activate IFG as parser of harmonic
138 regularities and top-down generator of predictions. On the other hand, we expected to find
139 divergent activity in temporal auditory or parietal visual-motor regions associated with item
140 identification and storage of knowledge in their modality-specific format. Finally, by
141 mirroring task-based activation (Smith et al., 2009), the resting-state data should reveal

142 processing streams involved in processing harmonic regularities in music perception and
143 action.

144

145 **2. Materials and methods**

146 **2.1 Participants.**

147 29 pianists (17 female) aged 20-32 years (mean age: 24.7, SD = 2.9) took part in the
148 experiment. They had a minimum of 5 years of piano training in classical Western tonal
149 music (range = 5 - 27 years, mean years of training = 17.2, SD = 4.8) and had started to play
150 the piano at an average age of 7.3 years (SD = 3.08). None of the pianists had training in
151 improvisation or other musical styles. All participants were naïve with regard to the purpose
152 of the study. Written informed consent was obtained from each participant before the study
153 that was approved by the local ethics committee.

154 **2.2 Stimuli.**

155 Stimuli (see Fig. 1) consisted of 60 different chord sequences that were presented as
156 piano sounds in the listening task (similar to Koelsch, 2005), and as photos of a hand playing
157 chords on a piano in the action imitation task (Bianco et al., 2016). The sequences were
158 composed of 5 chords according to the rules of classical harmony and had various melodic
159 contours. The first chord always represented the tonic (based on the first degree of the scale
160 in the relevant musical key). The second chord could be tonic, mediant (based on the third
161 scale degree) or subdominant (based on the fourth scale degree). Chords at the third position
162 were subdominant, dominant, or dominant six-four chords, and chords at the fourth position
163 were dominant seventh chords. At the last position, the target chord of each sequence was
164 manipulated in terms of harmonic congruency (CONG), so that the last chord could be either
165 congruent (a Tonic chord typically used to resolve a musical sequence) or incongruent (a
166 Neapolitan chord that sounds normal when played in isolation but constitutes a violation
167 when used at the end of a standard harmonic progression). Both the Tonic and Neapolitan are
168 consonant major chords built on the 1st and lowered 2nd scale degree, respectively (i.e., A for
169 Tonic and Bb for Neapolitan in A-major). Consequently, and due to the relationship of the
170 tonalities within the circle of fifths, the exact same chord that acts as a Tonic in one tonality
171 (e.g., A – #C – E in A-major), acts as a Neapolitan in another tonality (i.e., Bbb (=A) – Db (= #C) – Fb (= E) in Ab-major). We exploited this relationship and presented five sequences
173 from each of six different tonalities (D, E, Bb, Ab, A and Eb major), such that the majority of
174 final chords were presented as both Tonic and Neapolitan across the experiment. Therefore,
175 potential neural differences in processing congruent and incongruent chords cannot be due to
176 chord identity but more likely reflect harmony-related processes. With regard to the stimuli of
177 the action block, the choice of different tonalities further allowed us to balance the visual
178 appearance (i.e., number of black/white keys) and difficulty of execution of the target chord
179 (i.e., movement distance from second last to target chord) in congruent and incongruent
180 conditions (for visual appearance: average of 1.3 ± 0.5 black keys in the congruent and $1.2 \pm$

181 0.7 in the incongruent chords; for difficulty: average of 1 ± 0 key distance in the congruent
182 and 1.5 ± 0.2 in the incongruent sequences). All sequences were played with normal fingering
183 that was rated as being similarly conventional for congruent and incongruent endings (see
184 Bianco et al., 2016).

185 The audio stimuli were created with Logic Pro 8 (Apple Inc.), normalised for loudness
186 (RMS, root mean square) with Adobe Audition CS 6 and had a total duration of 6 seconds (1
187 second for each of the first four chords and 2 seconds for the target chord). In the action
188 block, the same chord sequences were presented as photo series showing a male pianist's
189 right hand pressing three keys forming each chord on a piano in conventional fingering
190 (Yamaha Clavinova CLP150, Yamaha Music Europe GmbH, Rellingen, Germany). Red
191 circles were superimposed on top of each pressed key (cf. Bianco et al, 2016) for the whole
192 duration of the photo to facilitate the recognition of the pressed keys. Each photo was
193 presented for 2 seconds (total sequence duration: 10 seconds).

194 **2.3 Procedure.**

195 The experimental session started with 14 minutes resting state fMRI data acquisition in
196 which participants were instructed to keep their eyes open and not to fall asleep. To prevent
197 any task-related bias in the measures of functional connectivity, pianists were asked not to
198 practice piano on the scanning day. Thereafter, the task session started and lasted for
199 approximately 25 minutes.

200 In the scanner, participants were required to imitate musical actions or to listen to
201 musical sequences in two separate blocks with a counterbalanced order across the group
202 (Fig.1). Stimulus presentation was controlled in an event-related design with Presentation
203 software (version 14.9, Neurobehavioural Systems, Inc.). In both blocks, congruent and
204 incongruent sequences were intermixed in a way that no more than 3 sequences of the same
205 condition followed each other. The inter-trial interval (ITI) ranged from 3 to 9 seconds and
206 during this period participants saw a black screen. During action imitation, no sound was
207 played. Pianists were asked to watch the performing hand in the photos and to simultaneously
208 copy the presented hand postures on a 5×15 cm² glass-board with their right hand (Fig.1, left
209 panel). To motivate participants to follow the sequence accurately, they were told that their
210 performance was monitored with a camera (MR-compatible camera, 12M camera, MRC
211 Systems, Heidelberg Germany). Since it is a common way for pianists to mentally practice by
212 motorically simulating piano performance, the playing along was meant to maximally involve
213 the motor system during the processing of musical actions. In the audio block, pianists were
214 asked to carefully listen to the sequences without playing along (Fig.1, right panel).

215 Only to ensure that participants paid attention to the stimuli and to assess their
216 awareness of the violations, 10 trials (1/6 of the trials) in both tasks were followed by a
217 prompt that asked participants to judge the harmonic correctness of the last presented
218 sequence. The judgement required a button response performed with the index or middle
219 finger of the left hand (key assignment was counterbalanced across participants). These

220 judgement trials were equally distributed over congruent and incongruent trials, and required
221 50% yes and 50% no responses.

222 After the scanning session, participants filled out a questionnaire to assess the degree to
223 which they had imagined the sound of the chord sequences during the action imitation task
224 and the movements to produce the sequences during the listening task.

225 -----

226 Figure 1

227 -----

228 **Figure 1.** Experimental design: expert pianists were presented with harmonically congruent
229 or incongruent chord progressions, presented either as muted musical actions (photos of a
230 hand playing chords) that they were required to imitate on a glass-board (left panel), or in an
231 auditory format that they listened to (right panel).

232 **2.4 Data acquisition.**

233 The experiment was carried out on a 3.0-Tesla Siemens TIM Trio whole body
234 magnetic resonance scanner (Siemens AG, Erlangen, Germany) using a 32-radiofrequency-
235 channel head coil. Functional magnetic resonance images were acquired using a T2*-
236 weighted 2D echo planar imaging (EPI) sequence. During 14 minutes of acquisition (TE =
237 36.5 ms, TR = 1400 ms) at rest (eyes open, instructed not to fall asleep) 410 volumes were
238 acquired with a square FOV of 64 axial slices of 2.3 mm thickness and no gap (2.3 x 2.3 x 2.3
239 mm³ voxel size) with a flip angle of 69°. Functional images during the two tasks were
240 acquired using an EPI sequence with TE = 30 ms and TR = 2000 ms. 456 and 377 volumes
241 were acquired in the action and audio block, respectively, with a square FOV of 210 mm,
242 with 37 interleaved slices of 3.2 mm thickness and 15% gap (3 x 3 x 3.68 mm³ voxel size)
243 aligned to the AC-PC plane, and a flip angle of 77°. For anatomical registration, high-
244 resolution T1-weighted images were acquired using a 3D MP2RAGE sequence (TI₁ = 700 ms,
245 TI₂ = 2500 ms, TE = 2.03 ms, TR = 5000 ms) with a matrix size of 240 x 256 x 176, with 1
246 mm isotropic voxel size, flip angle₁ of 4°, flip angle₂ of 8°, and GRAPPA acceleration factor
247 of 3.

248 **2.5 Data analysis.**

249 **2.5.1 Task-based fMRI**

250 fMRI data of 29 participants were analysed with statistical parametric mapping (SPM8;
251 Welcome Trust Centre for Neuroimaging; <http://www.fil.ion.ucl.ac.uk/spm/software/spm8/>)
252 using standard spatial pre-processing procedures. These consisted of: slice time correction (by
253 means of cubic spline interpolation method), spatial realignment, co-registration of functional
254 and anatomical data (uniform tissue-contrast image masked with the 2nd inversion image
255 from the MP2RAGE sequence), spatial normalisation into the MNI (Montreal Neurological
256 Institute) stereotactic space, that included resampling to 2x2x2 mm voxel size. Finally, data
257 were spatially low-pass filtered using a 3D Gaussian kernel with full-width at half-maximum

258 (FWHM) of 8 mm and temporally high-pass filtered with a cut-off of 1/128 Hz to eliminate
259 low-frequency drifts.

260 Statistical parametric maps for the whole brain data were generated in the context of
261 the general linear model (GLM) separately for the action imitation and the listening task. The
262 evoked hemodynamic response to the onset of the final chord was modelled for the congruent
263 and incongruent conditions as boxcars convolved with a hemodynamic response function
264 (HRF). To this design, we added estimated motion realignment parameters as covariates of no
265 interest to regress out residual motion artefacts and increase statistical sensitivity. To identify
266 hemodynamic responses related to the processing of harmonic violations, we computed the
267 first level contrast CONG (i.e., incongruent > congruent chords), separately for the action
268 imitation and the listening task. For random effects group analyses, the resulting contrast
269 images were submitted to one-sample *t*-tests. Additionally, to identify areas that are modality-
270 specific to either action or audio representation of the harmonic structure, we compared the
271 CONG contrasts of the two tasks by means of paired *t*-tests. We controlled family-wise error
272 rate (FWER) of clusters below 0.05 with a cluster-forming height-threshold of 0.001.
273 Anatomical labels are based on Harvard-Oxford cortical structural atlas implemented in FSL
274 (<http://neuro.debian.net/pkg/fsl-harvard-oxford-atlases.html>).

275 **2.5.2 Resting-state fMRI**

276 In order to investigate intrinsic connectivity of the peak regions from task-based fMRI
277 datasets (Bressler and Menon, 2010), independent resting state fMRI datasets were obtained
278 from 28 of the pianists that participated in the task-fMRI session (one r-fMRI data set was not
279 acquired due to technical problems). The pre-processing of the resting state data (realignment,
280 unwarping, slice-timing correction) was done using SPM8 by means of DPARSF
281 (<http://rfmri.org/DPARSF>) SPM-based toolboxes. We applied a GLM to regress out non-
282 neuronal signal changes due to physiological noise and, most importantly, head motions. The
283 regressors included six rigid-body motion parameters, five principle components extracted by
284 the “anatomical CompCor” (Behzadi et al., 2007) (i.e., signal from white matter and cerebral
285 fluid masks defined from anatomical scans), and finally global signal (Power et al., 2015).
286 Thereafter, band-pass-filtering (0.009 and 0.08 Hz), spatial normalization of functional data
287 into MNI stereotactic space (with resampling to 2 x 2 x 2 mm³ resolution), and finally a
288 minimal spatial smoothing with the FWHM of 3 mm were applied to the residual time-series.

289 Resting-state functional connectivity (RSFC) was defined by Pearson’s correlations
290 between a time-series of a seed region and time-series of whole brain voxels. Spherical seed
291 regions (5 mm radius) were centred in IFG at the peak coordinates of the CONG contrasts
292 obtained in the task-based analyses of the action imitation and the listening task. In order to
293 match the smoothness of noise in task-based and resting-state analyses, the correlation maps
294 were further smoothed with the FWHM of 2 mm, resulting in an effective FWHM of about
295 8 mm.

296 Voxel-wise paired t-tests were performed to identify differences between the two seed-
297 based correlation maps (i.e., action and audio seeds). The normality assumption based upon
298 the difference between the two correlation coefficients across subjects was fulfilled, as
299 confirmed by Kolmogorov-Smirnov tests. We controlled FWER of clusters below 0.05 with a
300 cluster-forming height-threshold of 0.001 in all reported results. Harvard-Oxford cortical
301 structural atlas was used to assign anatomical labels.

302

303 **3. Results.**

304 **3.1 Behavioural.**

305 To ensure that participants paid attention to the stimuli in both modalities and that they
306 were generally able to recognise the harmonic structure underlying the sequences, they were
307 required to overtly judge harmonic congruency in 1/6 of the trials. They performed
308 significantly above chance level in these explicit judgments both in the action (mean \pm *SD*:
309 68.96 \pm 27.06% correct, $p < .001$) and in the audio block (mean \pm *SD*: 91.03 \pm 16.40%
310 correct, $p < .001$), as tested with one-sample *t*-tests against 50% chance level. Action block
311 performance was lower than audio block performance ($t(28) = 4.704$, $p < .001$), partly due to a
312 response bias towards “congruent” answers in the action block (32% of incongruent trials
313 misclassified as congruent vs. 15% of congruent trials misclassified as incongruent: $t(28) =$
314 2.95, $p = 0.007$). These differences in explicit judgment might indicate that pianists were less
315 consciously aware of the harmonic violations during action imitation than during passive
316 listening, possibly because it is more taxing to copy sequences of actions on-line than to just
317 listen. This may have led pianists to focus on the motor-executive task rather than harmonic
318 relationships in the action block (see Discussion).

319 **3.2 fMRI.**

320 **3.2.1 Fronto-parietal vs. fronto-temporal areas for musical action vs. perception.**

321 In the action imitation task, the CONG contrast (incongruent vs. congruent chords)
322 yielded larger hemodynamic responses in frontal and parietal areas, comprising the dorsal
323 portion of rIFG (BA44) bordering precentral sulcus, and bilateral clusters extending from
324 superior parietal cortex (SPL: BA7) to the inferior parietal and middle occipital gyrus (MOG:
325 BA19) (Fig. 2 left-upper panel, Table 1).

326 In the listening task, the same contrast evoked stronger activity in frontal and temporal
327 areas, including right IFG (BA44/45, peak in ventral BA45) and the right posterior superior
328 temporal gyrus and sulcus (pSTG/STS: BA22) (Fig. 2 right-upper panel, Table 1).

329

330 -----

331 Figure 2

332 -----

333

334 **Figure 2.** Harmonic violations elicited activations in fronto-parietal areas during action
 335 imitation (upper left panel) and in fronto-temporal areas during listening (upper right panel).
 336 Areas involved in structural processing specifically for the action and the audio sequences
 337 were identified in bilateral posterior parietal regions (cold colours) and in bilateral temporal
 338 regions (hot colours), respectively (lower panel).
 339

Table 1. Congruency effect (incongruent > congruent) in the action imitation and listening tasks.

| Region | Hem. | BA | k | x | y | z | Z-value |
|--|------|--------|------|-----|-----|-----|---------|
| <i>Action: CONG incongruent > congruent</i> | | | | | | | |
| Precentral/Inferior Frontal Gyrus | R | 44 | 182 | 44 | 6 | 26 | 4.29 |
| | | 44 | | 64 | 18 | 24 | 3.53 |
| | | 44 | | 54 | 14 | 16 | 3.49 |
| Middle Occipital Gyrus | R | 19 | 352 | 40 | -80 | 36 | 4.66 |
| Superior Parietal Lobe | R | 7P | | 32 | -78 | 42 | 4.32 |
| Superior Parietal Lobe | L | 7P | 510 | 16 | -70 | 58 | 3.54 |
| | | 7P | | -16 | -74 | 58 | 4.27 |
| | | 7P | | -20 | -70 | 50 | 3.97 |
| Middle Occipital Gyrus | L | 19 | | -30 | -80 | 34 | 3.72 |
| <i>Audio: CONG incongruent > congruent</i> | | | | | | | |
| Inferior Frontal Gyrus | R | 45 | 1667 | 44 | 34 | 2 | 5.12 |
| | | 45 | | 44 | 18 | 16 | 4.98 |
| | | Insula | | 36 | 10 | -2 | 4.49 |
| Superior Temporal Sulcus, pos | R | 22 | 256 | 48 | -32 | 0 | 3.92 |
| Superior Temporal Gyrus, pos | R | 22 | | 70 | -24 | 6 | 3.59 |
| | | 22 | | 60 | -34 | 8 | 3.46 |
| Cerebellum (Crus II) | L | - | 132 | -14 | -76 | -36 | 4.37 |

340 Whole-brain activation cluster sizes (k), MNI coordinates (x, y, z), and Z-scores for
 341 the CONG contrast in action imitation and listening tasks ($p_{\text{voxel}} < .001$; $p_{\text{cluster}} < .05$,
 342 FWE corrected). BA: Brodmann area, Hem.: hemisphere.

343

344 To identify areas exclusively recruited depending on stimulus format (photos of actions
 345 or audio), the CONG contrasts of both tasks were compared using a paired *t*-test (Table 2).
 346 Incongruent actions elicited greater activity in bilateral SPL, MOG, and in the left
 347 superior/middle frontal gyrus (frontal eye fields, FEF: BA8) (Fig. 2 lower panel, cold
 348 colours). Conversely, auditory violations yielded larger BOLD responses in bilateral
 349 STS/STG, compared to the action task (Fig. 2 lower panel, hot colours).

350 To identify areas commonly recruited during both audio and action task, we masked
 351 the audio CONG contrast with the action contrast. This analysis yielded a cluster in rIFG
 352 (BA44, $x = 64$, $y = 18$, $z = 24$, cluster extent = 28 voxels, $Z = 3.53$, $p_{\text{voxel}} < .001$) that,
 353 however, did not survive the cluster-level FWER correction.

354

Table 2. *t*-test between the CONG contrasts in the action imitation and listening task.

| Region | Hem. | BA | k | x | y | z | Z-value |
|--------------------------|------|----|-----|----|-----|----|---------|
| <i>Action > Audio</i> | | | | | | | |
| Superior Parietal Lobe | R | 7 | 806 | 26 | -76 | 46 | 4.46 |

| | | | | | | | |
|--------------------------------|---|-------|------|-----|-----|----|------|
| | | 7 | | 24 | -58 | 44 | 4.22 |
| Middle Occipital Gyrus | R | 19 | | 34 | -80 | 38 | 4.08 |
| Middle Occipital Gyrus | L | 19 | 1436 | -32 | -76 | 24 | 4.99 |
| Superior Parietal Lobe | L | 7 | | -30 | -74 | 36 | 4.75 |
| | | 7 | | -20 | -72 | 48 | 4.41 |
| Superior Frontal Gyrus | L | 8 | 186 | -20 | 2 | 60 | 3.97 |
| | | 8 | | -22 | -2 | 72 | 3.60 |
| <i>Audio > Action</i> | | | | | | | |
| Superior-Middle Temporal Gyrus | R | 21/22 | 1100 | 64 | -16 | 8 | 4.79 |
| | | | | 62 | -32 | 4 | 4.64 |
| | | | | 52 | -30 | -8 | 4.20 |
| Superior-Middle Temporal Gyrus | L | 21/22 | 166 | -52 | -32 | -2 | 4.11 |
| | | | | -52 | -16 | 2 | 3.91 |
| | | | | -62 | -30 | 6 | 3.51 |

355 Whole-brain activation cluster sizes (k), MNI coordinates (x, y, z), and Z-scores for
356 the paired-samples *t*-test comparison of the action > audio and audio > action CONG
357 contrast ($p_{\text{voxel}} < .001$; $p_{\text{cluster}} < .05$, FWE corrected. BA: Brodmann area, Hem.:
358 hemisphere.

359

360 3.2.2 Seed-based functional connectivity from the IFG peak maxima.

361 To gather evidence for the communication between IFG and modality-specific areas,
362 we conducted a seed-based functional connectivity analysis on the resting-state fMRI data
363 acquired from the same pianists. The activation peaks in the IFG clusters in the action
364 imitation and audio task were chosen as seed regions, which were located between the right
365 dorsal BA44 and the pre-central sulcus (action-seed) and in right BA45 (audio-seed). The
366 results are depicted in Figure 3 (upper and middle panels) and show positive functional
367 connectivity (hot colours) between IFG and (amongst others) regions that were functionally
368 specific to the action or audio musical task.

369

370 -----

371 Figure 3

372 -----

373

374 **Figure 3.** *Upper and middle panels:* seed-based functional connectivity maps on resting-state
375 data from the action seed in dorsal BA44 and audio seed in ventral BA45, respectively. Seeds
376 are depicted as black circles. Hot and cold colours indicate positive and negative functional
377 connectivity, respectively. Consistent with the task-based activations, the topographical
378 connectivity patterns include posterior parietal regions from the action-seed and temporal
379 regions from the audio-seed. *Lower panel:* *t*-test between the connectivity maps of the action-
380 and audio seed. Correlation values in posterior parietal areas were significantly higher for the
381 action-seed than the audio-seed, whereas temporal regions were more strongly correlated to
382 the audio- than the action-seed.

383

384 In line with activity in IFG and posterior parietal regions in the action task, the action-
385 seed in IFG (BA44) exhibited positive correlations within a dorsal motor network comprising
386 bilateral parietal cortex, extending from the anterior ventral supramarginal gyrus (BA40) to
387 the posterior superior parietal lobes (BA7) (Table 3). Notably, there were no significant
388 correlations with temporal regions that were specific to the audio modality. A large cluster
389 peaking in bilateral precentral gyrus showed positive correlations with the action-seed,
390 including subclusters in bilateral BA44 extending to insular regions, ventral premotor cortex
391 (BA6), middle frontal gyrus (BA9) bordering the superior frontal gyrus and the inferior
392 portion of the frontal pole (BA10). Medially, the action seed exhibited positive correlations
393 with the right posterior border of the supplementary motor cortex (BA6) and anterior
394 cingulate (BA24). Finally, there were positive correlations with right inferior temporal gyrus
395 at the temporo-occipital junction (BA20), and bilateral occipitotemporal areas (BA37),
396 cerebellum and thalamus.

397 Consistent with activity in IFG and temporal areas in the audio task, the audio-seed in
398 IFG (BA45) exhibited positive correlations within the auditory network comprising the
399 posterior part of the right superior temporal gyrus (BA22) and left Heschl's gyrus (including
400 BA41/42) (Table 3). Additionally, there were positive correlations with frontal areas in the
401 right hemisphere including orbitofrontal (BA47/11/12) and frontopolar regions (BA10),
402 superior (BA8), middle frontal areas (BA9), and anterior cingulate gyrus (BA24), and in the
403 left hemisphere, including BA45, BA47, BA9, BA10, and BA12. In the parietal cortex,
404 positive correlations were restricted to bilateral anterior ventral supramarginal gyrus (BA40),
405 without extending to more posterior parietal regions. Finally, there were positive correlations
406 with thalamus and right putamen.

407 Apart from positive correlations, activity in both action and audio seeds was negatively
408 correlated (Figure 3 upper and middle panels, cold colours) with activity in areas belonging to
409 the default mode network (DMN), namely the cingulate gyrus and the superior portion of
410 bilateral lateral occipital cortex extending into angular gyrus. These regions typically show a
411 decrease of activation during attention-demanding tasks and goal-directed behaviours (Uddin
412 et al., 2009). Additionally, negative correlations were found between the action-seed and
413 bilateral anterior middle temporal gyrus and medial prefrontal cortex, anti-correlations that
414 have been associated with highly difficult goal-directed tasks, as could apply in the case of
415 our action-task (McKiernan et al., 2003).

416 Finally, a paired-samples *t*-test comparing the connectivity maps of the action- and
417 audio-seed (Table 4) confirmed their differential predominant connectivity to parietal and
418 temporal areas, respectively. Specifically, connectivity of the action-seed (compared to audio-
419 seed) was stronger to bilateral posterior parieto-occipital areas, as well as to bilateral
420 cerebellum, right frontal pole, frontal medial cortex and anterior cingulate gyrus, left superior
421 frontal and precentral gyrus. Conversely, the connectivity of the audio-seed (compared to
422 action-seed) was stronger to bilateral superior or middle temporal gyrus, as well as to bilateral

423 cerebellum, right superior frontal gyrus, posterior cingulate and angular gyrus, thalamus, and
424 left frontal operculum.

Table 3. Resting-state functional connectivity from the action and audio seed in right inferior frontal gyrus.

| Region | BA | Action-seed | | | | | Audio-seed | | | | |
|---|----------|-------------|-----|-----|-----|---------|------------|-----|-----|-----|---------|
| | | k | x | y | z | Z-value | k | x | y | z | Z-value |
| <i>Right Hemisphere (positive correlations)</i> | | | | | | | | | | | |
| Frontal Pole | 10 | 125 | 26 | 38 | -16 | 4.94 | | | | | |
| Middle Frontal Gyrus | 9 | | | | | | 310 | 42 | 4 | 46 | 5.22 |
| Superior Frontal Gyrus | 8 | | | | | | 349 | 4 | 18 | 60 | 4.79 |
| Supplementary Motor Cortex | 6 | 734 | 6 | 14 | 52 | 5.92 | | | | | |
| Cingulate Gyrus, ant. | 24 | 133 | 4 | 6 | 28 | 5.76 | 324 | 4 | 32 | 22 | 4.86 |
| Supramarginal Gyrus/Superior Parietal Lobe | 40/7 | 5418 | 52 | -30 | 48 | 6.89 | | | | | |
| Superior Temporal Gyrus, post | 22 | | | | | | 119 | 50 | -14 | -8 | 4.33 |
| Superior Temporal Gyrus, post. | 22 | | | | | | 1148 | 52 | -30 | 6 | 4.72 |
| Middle temporal Gyrus | 20/21/37 | 1304 | 52 | -56 | -12 | 5.92 | | | | | |
| Putamen | - | | | | | | 36 | 32 | -12 | -8 | 4.52 |
| Thalamus | - | 120 | 8 | -14 | 8 | 5.84 | | | | | |
| Cerebellum (VIIb) | - | 350 | 18 | -68 | -48 | 5.36 | | | | | |
| Cerebellum (VI) | - | 95 | 8 | -70 | -22 | 4.98 | | | | | |
| <i>Left Hemisphere (positive correlations)</i> | | | | | | | | | | | |
| Frontal Pole | 10 | 531 | -44 | 38 | 8 | 6.28 | | | | | |
| Frontal Operculum Cortex | 45 | | | | | | 2198 | -38 | 26 | 0 | 6.29 |
| Inferior Frontal Gyrus | 44 | | | | | | 50 | -46 | 12 | 22 | 4.29 |
| Precentral Gyrus | 6/44/Ins | 2415 | -44 | 6 | 24 | 6.89 | | | | | |
| Middle Frontal Gyrus | 9 | 626 | -26 | 0 | 50 | 6.15 | | | | | |
| Cingulate Gyrus, ant. | 24 | | | | | | 52 | -2 | -12 | 42 | 3.98 |
| Heschl's Gyrus (H1 and H2) | 41/42 | | | | | | 173 | -52 | -14 | 4 | 4.07 |
| Supramarginal Gyrus/Superior Parietal Lobe | 40/7 | 3814 | -60 | -30 | 42 | 5.92 | 143 | -66 | -38 | 26 | 4.21 |
| Middle temporal Gyrus | 20/21/37 | 1162 | -60 | -60 | -6 | 5.60 | 63 | -62 | -60 | 8 | 4.03 |
| Thalamus | - | 116 | -12 | -14 | 6 | 4.45 | 93 | -6 | -14 | 2 | 5.43 |
| Cerebellum (VIIb) | - | 969 | -26 | -66 | -52 | 6.06 | | | | | |
| Cerebellum (VI) | - | 95 | -22 | -62 | -28 | 4.98 | | | | | |
| Cerebellum (Crus II) | - | | | | | | 58 | -16 | -78 | -34 | 4.40 |

| | | | | | | | | | | | |
|---|----|-------|-----|-----|-----|-------|------|-----|-----|-----|------|
| <i>Right Hemisphere (negative correlations)</i> | | | | | | | | | | | 425 |
| | | | | | | | | | | | 426 |
| Frontal Pole | 10 | 11860 | 6 | 60 | 22 | 7.08 | | | | | |
| Superior Frontal Gyrus | 8 | | | | | | 384 | 28 | 30 | 54 | 4.97 |
| Middle Temporal Gyrus | 21 | 2367 | 60 | 4 | -24 | 6.88 | | | | | |
| Cingulate Gyrus, pos. | 24 | 5798 | 10 | -50 | 34 | 7.66 | 3682 | 10 | -46 | 12 | 5.35 |
| Cerebellum (IX) | - | 187 | 4 | -50 | 44 | 5.81 | | | | | |
| Cerebellum (Crus I) | - | 1799 | 26 | -88 | -30 | 5.99 | 326 | 36 | -52 | -34 | 4.99 |
| <i>Left Hemisphere (negative correlations)</i> | | | | | | | | | | | |
| Frontal Pole | 10 | | | | | | 105 | -20 | 64 | -6 | 4.37 |
| Superior Frontal Gyrus | 8 | | | | | | 601 | -20 | 28 | 38 | 5.67 |
| Middle Temporal Gyrus | 21 | 2367 | -62 | -24 | -12 | 6.88 | | | | | |
| Inferior Temporal Gyrus, pos. | 20 | | | | | | 70 | -60 | -44 | -14 | 4.17 |
| Lateral Occipital Cortex, sup. | 39 | 1764 | -40 | -50 | 26 | 6.27 | 1268 | -36 | -66 | 38 | 5.57 |
| Hippocampus | - | 62 | -34 | -34 | -8 | 5.01 | 65 | -30 | -34 | -12 | 4.07 |
| Cerebellum (Crus I) | - | 27 | -44 | -56 | -42 | 4.275 | | | | | |

Results of the whole-brain functional connectivity analysis from IFG activation maxima in action imitation and listening tasks. BA: Brodmann area, k: cluster size, MNI coordinates (x, y, z), and Z scores. ($p_{\text{voxel}} < .001$; $p_{\text{cluster}} < .05$, FWE corrected).

Table 4. Comparison of rs-functional connectivity from the action- and audio-seed in the right IFG.

| Region | BA | Action > Audio seed | | | | | Audio > Action seed | | | | |
|------------------------------------|-------|---------------------|-----|-----|-----|---------|---------------------|-----|-----|-----|---------|
| | | k | x | y | z | Z-value | k | x | y | z | Z-value |
| <i>Right Hemisphere</i> | | | | | | | | | | | |
| Frontal Pole | 10 | 93 | 48 | 42 | 14 | 3.56 | | | | | |
| Superior Frontal Gyrus | 9 | | | | | | 4263 | 4 | 56 | 42 | 5.28 |
| Frontal medial cortex | 11 | 59 | 4 | 44 | -18 | 3.88 | | | | | |
| Cingulate Gyrus | 23/24 | 52 | 2 | 6 | 30 | 4.58 | 200 | 2 | -14 | 38 | 4.89 |
| Superior Temporal Gyrus | 22 | | | | | | 645 | 52 | -8 | -8 | 5.16 |
| Angular Gyrus | 40 | | | | | | 161 | 44 | -46 | 32 | 4.20 |
| Lingual Gyrus | 27 | 72 | 16 | -42 | -6 | 4.87 | | | | | |
| Infer. Temporal Gyrus, temp-occ.j. | 37 | 996 | 52 | -56 | -14 | 5.53 | | | | | |
| Lateral Occipital Cortex, sup. | 7 | 4448 | 24 | -68 | 50 | 6.03 | | | | | |
| Precuneus Cortex | 17 | 373 | 24 | -54 | 18 | 4.80 | | | | | |
| Thalamus | - | | | | | | 50 | 2 | -12 | 10 | 4.49 |
| Cerebellum (Crus II) | - | 153 | 4 | -78 | -44 | 4.24 | 68 | 30 | -88 | -36 | 3.86 |
| Cerebellum (XI) | - | 51 | 16 | -46 | -48 | 4.46 | | | | | |
| <i>Left Hemisphere</i> | | | | | | | | | | | |
| Frontal Operculum Cortex | 47 | | | | | | 976 | -40 | 26 | 0 | 5.35 |
| Superior Frontal Gyrus | 8 | 640 | -24 | 4 | 52 | 5.17 | | | | | |
| Precentral gyrus | 6 | 549 | -52 | 6 | 40 | 5.43 | | | | | |
| Middle Temporal Gyrus (middle) | 20 | | | | | | 206 | -56 | -20 | -12 | 4.88 |
| Middle Temporal Gyrus (post.) | 21 | | | | | | 64 | -54 | -38 | 0 | 4.38 |
| Temporal Occipital Fusiform Cortex | 7 | 66 | -24 | -58 | -12 | 4.10 | | | | | |
| Lateral Occipital Cortex, sup. | 7 | 3678 | -26 | -76 | 30 | 5.66 | | | | | |
| Lateral Occipital Cortex, inf. | 19 | 567 | -50 | -76 | -4 | 4.87 | | | | | |
| Cerebellum (Crus I/II) | - | 114 | -6 | -76 | -40 | 4.30 | 168 | -24 | -76 | -34 | 4.44 |

428 Results of the *t*-test between whole-brain functional connectivity from IFG activation maxima in action imitation and
429 listening task. BA: Brodmann area, k: cluster size, MNI coordinates (x, y, z), and Z scores. ($p_{\text{voxel}} < .001$; $p_{\text{cluster}} < .05$,
430 FWE corrected). temp-occ.j.: temporo-occipital junction.

431 **4. Discussion**

432 The present study investigated the neural bases of action planning and prediction based on long-
433 term knowledge of harmonic regularities and compared them with those involved in auditory prediction.
434 Functional neuroimaging data of expert pianists were acquired at rest, during imitation of (without sound)
435 or listening to (without imitation) harmonically congruent or incongruent chord sequences presented as
436 photos of musical actions or sounds, respectively. Violations in both musical *actions* and *sounds* recruited
437 distinct sub-regions (BA 44 and BA 45, respectively) in right IFG (rIFG) interconnected with parietal
438 visual-motor and temporal auditory areas, respectively. We propose that motoric and auditory long-term
439 representations of harmonic regularities are likely to account for the differential involvement of parietal
440 and temporal areas that enter into dynamic interactions with computations in rIFG. Moreover, the
441 involvement of rIFG in parsing musical action and sound sequences is sensitive to stimulus properties and
442 task – production or perception – accounting for the divergent peak localizations, in line with prevailing
443 models of general prefrontal cortex organization (e.g., Fuster, 2001), and dual stream models of the visuo-
444 spatial (e.g., Goodale & Milner, 1992) and auditory system (e.g., Rauschecker and Scott, 2009).
445 Altogether, our results emphasise dissociable, neural action and audio networks in which modality-
446 specific long-term knowledge and contextual information act as priors for the prediction of forthcoming
447 events. In this respect, predictive coding models (Friston, 2010) may yield a unifying explanatory
448 framework for information processing across both action and perception.

449

450 **4.1 Musical action**

451 The imitation of incongruent actions elicited activations in fronto-parietal areas (see Table 1),
452 including the right inferior frontal gyrus (IFG: dorsal BA44 extending to the border of the precentral
453 sulcus) and bilateral posterior parietal cortex (pSPL: BA7; MOG: BA19).

454 This activation pattern resembles the typical dorsal fronto-parietal network for visually guided
455 behaviour that integrates sensory information with action-goals through sensorimotor transformations
456 (Gallivan and Culham, 2015; Kravitz et al., 2011). Accordingly, MOG is known as an area involved in
457 capturing relevant visual-spatial dimensions of objects and visually-guided actions (Lingnau and
458 Downing, 2015). SPL has been associated with high-level aspects of motor behaviour, such as the
459 formation of intentions and early movement plans. These processes are aided by critical operations of
460 multisensory integration and visuomotor transformation in SPL (Andersen and Buneo, 2002). Activations
461 in pSPL have been reported during motor imagery of action-goals and trajectories (Aflalo et al., 2015),
462 attentional spatial remapping/reprogramming of pre-selected actions (O'Reilly et al., 2013), and
463 transformation of spatial target information into corresponding actions (Barany et al., 2014; Schon et al.,
464 2002).

465 One crucial finding was the recruitment of the rIFG (dorsal BA44) when the final chord, predicted
466 by the harmonic structure of the given musical sequence, was violated. This is consistent with the role of
467 IFG in processing high-level aspects of motor behaviours (Grafton and Hamilton, 2007). Experimental

468 evidence emphasises the role of bilateral IFG in processing hierarchical relationships within action
469 sequences either when judging complex familiar activities (Farag et al., 2010) or when executing abstract
470 hierarchically organised patterns of action sequences (Koechlin and Jubault, 2006). Altogether, these
471 combined results suggest that the right IFG supports the structural integration of simple acts into more
472 complex combinatorial action sequences. The greater BOLD response during incongruent (compared to
473 congruent) chords may be due to a mismatch with the predicted musical motor act that leads to higher
474 computational costs during structural integration. Importantly, these findings indirectly show that pianists'
475 knowledge of harmonic regularities transfers to the motor domain and enables them to predict and plan
476 forthcoming musical acts during performance.

477 The absence of auditory activation in the incongruent vs. congruent contrast suggests that pianists
478 relied more on their action knowledge recalled by the execution of the preceding chords than on auditory
479 mechanisms (Bianco et al., 2016; Novembre and Keller, 2011; Sammler et al., 2013). Note that this
480 finding does not conflict with the large body of experimental evidence for action-perception coupling in
481 trained musicians (for review, see Novembre and Keller, 2014; Zatorre et al., 2007) Our unusual and
482 taxing imitation task on unrehearsed sequences may have led pianists to focus on the motor part of the
483 task, possibly suppressing unhelpful auditory images (cf. Pfordresher, 2012; van der Steen et al.,
484 2014)(cf. Pfordresher, 2012). Alternatively, auditory feed-forward mechanisms may not discriminate
485 between congruent and incongruent chords such that auditory activations cancelled out.

486 Overall, these fronto-parietal activations complement and support our previous behavioural
487 (Novembre & Keller, 2011) and EEG studies on expert pianists (Bianco et al., 2016; Sammler et al.,
488 2013): silent production of harmonically incongruent chords elicited response time costs and a centro-
489 parietal negativity that was associated with mechanisms of motor reprogramming of a pre-planned action
490 in face of the violation. The activations of SPL and MOG match and support our interpretation of the
491 posterior negativity as a correlate of the spatial remapping and reprogramming of pre-planned actions, and
492 the activation of IFG lends evidence that these mechanisms stand under frontal control.

493 Within the predictive-coding framework (Friston, 2010), a bidirectional flow of information can be
494 suggested to occur in the two hemispheres between parietal areas, processing visual-motor inputs, and the
495 IFG, performing structural integration of incoming items. Indeed, the functional connectivity analysis of
496 our resting state data revealed strong positive correlations between right BA44 and, amongst others,
497 bilateral superior parietal lobes, also revealed by the task-based analysis. A fronto-parietal network relying
498 on the route of the dorsal visual stream has been associated with sensorimotor transformation during
499 visually guided action planning (Goodale and Milner, 1992). According to motor control theory, these
500 operations might be supported by “forward models”, through which the expected outcome of an action is
501 compared with actual sensory feedback (Wolpert and Flanagan, 2001). In this framework, posterior
502 parietal regions simultaneously represent potential actions whose pre-selection is biased by the influence
503 of internal models from prefrontal regions (Cisek, 2006). The novel finding is that these internal models
504 may be shaped by the musician’s knowledge of harmonic regularities and musical context. We propose

505 that, on the one hand, visual-motor information about the current act is forwarded from posterior regions
506 to the IFG that integrates the items and builds up an internal model of the sequence's harmonic structure.
507 On the other hand, this internal model affords predictions of visual-spatial surface features of the next
508 chord in MOG and may bias the pre-selection/representation of harmonically appropriate forthcoming
509 motor acts in SPL. The generated model would be continually validated/updated via the matching between
510 the expected action and the combined visual and proprioceptive signals from the current input (Wolpert
511 and Flanagan, 2001). Interestingly, the combined findings raise the hypothesis that (musical) action
512 knowledge, internal visual-motor models and fronto-parietal information flow may provide the basis on
513 which the motor system contributes to visual perception and prediction of human behaviour (Novembre
514 and Keller, 2014).

515

516 **4.2 Music perception**

517 In line with previous findings (Koelsch et al., 2005), listening to harmonically incongruent
518 compared to congruent chords elicited activations in fronto-temporal areas: right inferior frontal gyrus
519 (IFG: BA44, BA45) extending into the insular cortex, and right posterior superior temporal gyrus and
520 sulcus (pSTG/STS: BA22).

521 The IFG and the posterior STG have been associated with structural analysis of auditory musical
522 sequences based on internalised knowledge of harmonic regularities (Koelsch et al., 2005; Maess et al.,
523 2001; Sammler et al., 2013a; Tillmann et al., 2006). The IFG has been proposed to support integration of
524 discrete items into higher-order structures, based on which top-down predictions on forthcoming items can
525 be generated. Greater BOLD responses in IFG may reflect the higher computational demand to integrate
526 incongruent chords that are weakly related to the harmonic context and do not fulfil the prediction.
527 Compared to these higher-order computations in IFG, pSTG/STS has been proposed to support lower-
528 level matching processes between the actually perceived and the predicted sensory information (Sammler,
529 Koelsch, et al., 2013). Indeed, posterior superior temporal areas have been associated with physical feature
530 analysis and short-term representation of sounds (Seger et al., 2013), as well as with the identification of
531 the harmonic functions of chords within musical sequences (Musso et al., 2015).

532 Our connectivity analysis showed a functional coupling between IFG (BA44/BA45) and
533 pSTG/STS, making it plausible to assume bidirectional dynamic fronto-temporal interactions during
534 structural integration processes (Friston, 2010). On the one hand, early sensory analysis of chord functions
535 may be forwarded from temporal to frontal regions where information is structurally integrated and
536 harmonic predictions are established. On the other hand, these predictions may in turn inform the
537 identification process in pSTG/STS where perceived and predicted items are matched to validate or revise
538 the frontal prediction.

539 Overall, these data emphasise the crucial role of not just one area, but of a dynamic exchange of
540 information between fronto-temporal areas in providing resources for the parsing of complex
541 harmonically organised sounds (Hyde et al., 2011). Neuroanatomically, the fronto-temporal information

542 exchange may be implemented along dorsal or ventral auditory pathways (see further below) (Loui et al.,
543 2011; Musso et al., 2015; Rauschecker, 2011). The anatomical specification of these pathways, their
544 functional relevance and dependency on musical training are interesting topics for future research.

545

546 **4.3 Dorsal and ventral streams for musical action and perception**

547 As discussed above, harmonic processing in musical actions and auditory perception relied on
548 dissociable fronto-parietal and fronto-temporal neural networks, respectively. Representations of harmonic
549 regularities in either visual-motor or auditory format are likely to account for the differential involvement
550 of parietal and temporal areas, respectively, that both dynamically interact with computational processes
551 in IFG. Interestingly, these interactions involved distinct posterior-dorsal and anterior-ventral rIFG sub-
552 regions, i.e., BA6/44 in the action imitation task vs. BA44/45 in the audio task. This dissociation may
553 either reflect (i) a task-unspecific sensitivity of IFG to structural processing demands in line with models
554 of general prefrontal cortex specialization, or (ii) a task-specific involvement of dorsal and ventral IFG
555 sub-regions as endpoints of different processing streams.

556 (i) Investigating harmonic structure processing in perception and action necessarily entails
557 differences in experimental setup that alone suffice to induce different processing demands and shift
558 activation peaks within IFG – even if both peaks may reflect similar structural computations. For example,
559 recent theories propose anterior-posterior (Badre and D’Esposito, 2009; Fuster, 2001; Koechlin and
560 Summerfield, 2007) and/or rostral-caudal (Friederici, 2011) gradients of prefrontal cortex organization
561 along which *similar* functions, e.g., the “integration” of discrete items over time, operate at *different* levels
562 of abstraction (Makuuchi et al., 2012). Along these lines, the more demanding imitation task might have
563 triggered integration over shorter segments in the action sequences (i.e., integration at a lower level of
564 complexity), limiting the activation to dorsal BA44 in the action contrast.

565 (ii) Alternatively, the divergence of dorsal and ventral rIFG peaks and connectivity profiles may
566 arise from the intrinsically different nature of the tasks – silent musical action imitation vs. listening – in
567 line with dual stream models of the visuo-spatial (Goodale and Milner, 1992; Kravitz et al., 2011) and
568 auditory system (Rauschecker and Scott, 2009; Rauschecker, 2011). According to these models, dorsal
569 portions of IFG are interconnected with the parietal and temporal lobe within dorsal processing streams
570 for time-dependent mechanisms that afford transformation between sensory input (visuo-spatial or sound)
571 and motor representations, thereby supporting action. Dorsal stream involvement has been shown
572 previously for goal-related actions (Kravitz et al., 2011), speech production (Hickok & Poeppel, 2007) and
573 singing (Loui, 2015; Zarate, 2013) and is compatible with our fronto-parietal network observed in pianists
574 during musical action imitation. Moreover, since the audio contrast comprised frontal activation extending
575 to dorsal IFG, it is plausible that also during listening (although without imitation) a dorsal stream of
576 auditory information might have been involved for mapping sound to action simulated by pianists (Zatorre
577 et al., 2007). Notably, the present study adds two new insights: first, we demonstrate that frontal and
578 parietal areas along the dorsal stream provide the neural resources for sequential structure processing

579 during production of musical sequences; second, unlike in singing or speech production, our action
580 imitation task eliminated auditory feedback during self-produced actions, hence, leading us to conclude
581 that music-structural predictions can be grounded in the visual-motor control system.

582 Ventral IFG, in turn, is known as endpoint of the auditory ventral stream that, in concert with
583 posterior temporal areas, is classically thought to process pitch information during singing (Berkowska
584 and Dalla Bella, 2009; Zarate, 2013) and to map sound to meaning (Hickok and Poeppel, 2007;
585 Rauschecker and Scott, 2009), compatible with our fronto-temporal network observed during listening.
586 Although musical harmony does not have referential meaning as language, harmonic incongruities do
587 have musical significance to listeners – i.e., intra-musical meaning as framed by Koelsch (2011) – in that
588 the harmonic context leads towards a target chord that can be classified as more or less appropriate for
589 musical closure.

590 Although the current findings do not speak to the causal role of the nodes or streams, they
591 altogether highlight the relevance of considering structural integration in music production and perception
592 as a network capacity by taking into account the connectivity between frontal computational and posterior
593 modality-specific regions. Flexible and proficient music performance is likely to benefit from the dynamic
594 weighting of these dissociable visual-motor and auditory circuits for prediction and motor planning based
595 on internalised knowledge of harmony.

596

597 **5. Conclusion**

598 The present data provide first neuroimaging evidence that expert pianists predict forthcoming
599 musical chords not only in auditory perception, but also in the processing of actions independently of
600 auditory information. Remarkably, this suggests that, after intensive training, knowledge of structural
601 regularities influences experts' action planning via implicit mechanisms of motor prediction/control, and
602 might in turn increase proficiency of performance on top of fine movement optimization.

603 Our paradigm, in which pianists acted without listening to sound and listened without acting,
604 dissociated a dorsal action and a ventral audio network for harmonic prediction, potentially acting in
605 concert during real production (i.e., playing with sound). The dorsal and ventral networks both involve
606 frontal computational sub-regions in rIFG, interconnected with parietal and temporal posterior systems of
607 knowledge, respectively. These networks are likely to provide the infrastructure that allows frontal areas
608 to keep track of abstract dependencies in sequential information via dynamic exchange with progressively
609 lower-level modality-specific systems of knowledge. Predictive coding is proposed as an explanatory
610 framework that unifies both networks' functional roles: to optimise predictions in action and perception
611 based on previous exposure and knowledge of harmony.

612

613 **Acknowledgments**

614 We are grateful to the pianists who participated in this experiment and to Bruno Pace who lent a
615 hand in stimulus preparation. We also thank Mauricio Martins, Tomás Goucha, Gabriele Chierchia and

616 Emiliano Zaccarella for inspiring discussions and Sven Gutekunst and Jöran Lepsien for technical support.
617 This research was funded by the Max Planck Society.

References

- Aflalo, T., Kellis, S., Klaes, C., Lee, B., Shi, Y., Pejsa, K., Shanfield, K., Hayes-jackson, S., Aisen, M., Heck, C., Liu, C., Andersen, R.A., 2015. Decoding motor imagery from the posterior parietal cortex of a tetraplegic human. *Science* (80-.). 348, 906–910.
- Andersen, R.A., Buneo, C.A., 2002. Intentional maps in posterior parietal cortex. *Annu. Rev. Neurosci* 25, 189–220.
- Badre, D., D’Esposito, M., 2009. Is the rostro-caudal axis of the frontal lobe hierarchical? *Nat. Rev. Neurosci.* 10, 659–669.
- Barany, D. a, Della-Maggiore, V., Viswanathan, S., Cieslak, M., Grafton, S.T., 2014. Feature interactions enable decoding of sensorimotor transformations for goal-directed movement. *J. Neurosci.* 34, 6860–73.
- Behzadi, Y., Restom, K., Liao, J., Liu, T.T., 2007. A component based noise correction method (CompCor) for BOLD and perfusion based fMRI. *Neuroimage* 37, 90–101.
- Berkowska, M., Dalla Bella, S., 2009. Acquired and congenital disorders of sung performance: A review. *Adv. Cogn. Psychol.* 5, 69–83.
- Bharucha, J., Krumhansl, C.L., 1983. The representation of harmonic structure in music: hierarchies of stability as a function of context. *Cognition* 13, 63–102.
- Bianco, R., Novembre, G., Keller, P.E., Scharf, F., Friederici, A.D., Villringer, A., Sammler, D., 2016. Syntax in Action Has Priority over Movement Selection in Piano Playing: An ERP Study. *J. Cogn. Neurosci.* 28, 41–54.
- Bressler, S.L., Menon, V., 2010. Large-scale brain networks in cognition: emerging methods and principles. *Trends Cogn. Sci.* 14, 277–290.
- Cisek, P., 2006. Integrated neural processes for defining potential actions and deciding between them: a computational model. *J. Neurosci.* 26, 9761–70.
- Eerola, T., Himberg, T., Toiviainen, P., Louhivuori, J., 2006. Perceived complexity of western and African folk melodies by western and African listeners. *Psychol. Music* 34, 337–371.
- Farag, C., Troiani, V., Bonner, M., Powers, C., Avants, B., Gee, J., Grossman, M., 2010. Hierarchical organization of scripts: Converging evidence from fmri and frontotemporal degeneration. *Cereb. Cortex* 20, 2453–2463.
- Fazio, P., Cantagallo, A., Craighero, L., D’Ausilio, A., Roy, A.C., Pozzo, T., Calzolari, F., Granieri, E., Fadiga, L., 2009. Encoding of human action in Broca’s area. *Brain* 132, 1980–8.
- Fiebach, C.J., Schubotz, R.I., 2006. Dynamic anticipatory processing of hierarchical sequential events : a common role for broca ’ s area and ventral premotor cortex across domains ? *Cortex* 42, 499–502.
- Fitch, W.T., Martins, M.D., 2014. Hierarchical processing in music, language, and action: Lashley revisited. *Ann. N. Y. Acad. Sci.* 1316, 87–104.
- Friederici, A.D., 2011. The brain basis of language processing: from structure to function. *Physiol. Rev.* 91, 1357–92.

- Friston, K., 2010. The free-energy principle: a unified brain theory? *Nat. Rev. Neurosci.* 11, 127–38.
- Fuster, J.M., 2001. The prefrontal cortex - An update: Time is of the essence. *Neuron* 30, 319–333.
- Gallivan, J.P., Culham, J.C., 2015. Neural coding within human brain areas involved in actions. *Curr. Opin. Neurobiol.* 33, 141–149.
- Goodale, M. a., Milner, A.D., 1992. Separate visual pathways for perception and action. *Trends Neurosci.* 15, 20–25.
- Grafton, S.T., Hamilton, A.F.D.C., 2007. Evidence for a distributed hierarchy of action representation in the brain. *Hum. Mov. Sci.* 26, 590–616.
- Hickok, G., Poeppel, D., 2007. The cortical organization of speech processing. *Nat. Rev. Neurosci.* 8, 393–402.
- Hyde, K.L., Zatorre, R.J., Peretz, I., 2011. Functional MRI evidence of an abnormal neural network for pitch processing in congenital amusia. *Cereb. Cortex* 21, 292–9.
- Kilner, J.M., Friston, K.J., Frith, C.D., 2007. Predictive coding: an account of the mirror neuron system. *Cogn. Process.* 8, 159–66.
- Kim, S.-G., Kim, J.S., Chung, C.K., 2011. The effect of conditional probability of chord progression on brain response: an MEG study. *PLoS One* 6, e17337.
- Koechlin, E., Jubault, T., 2006. Broca's area and the hierarchical organization of human behavior. *Neuron* 50, 963–74.
- Koechlin, E., Summerfield, C., 2007. An information theoretical approach to prefrontal executive function. *Trends Cogn. Sci.* 11, 229–35.
- Koelsch, S., 2011. Toward a neural basis of music perception - a review and updated model. *Front. Psychol.* 2, 110.
- Koelsch, S., 2005. Neural substrates of processing syntax and semantics in music. *Curr. Opin. Neurobiol.* 15, 207–12.
- Koelsch, S., Fritz, T., Schulze, K., Alsup, D., Schlaug, G., 2005. Adults and children processing music: an fMRI study. *Neuroimage* 25, 1068–76.
- Koelsch, S., Siebel, W. a, 2005. Towards a neural basis of music perception. *Trends Cogn. Sci.* 9, 578–84.
- Kravitz, D.J., Saleem, K.S., Baker, C.I., Mishkin, M., 2011. A new neural framework for visuospatial processing. *Nat. Rev. Neurosci.* 12, 217–30.
- Krumhansl, C.L., 1983. Perceptual structures for tonal music. *Music Percept.* 1, 28–62.
- Large, E.W., Palmer, C., 2002. Perceiving temporal regularity in music. *Cogn. Sci.* 26, 1–37.
- Lartillot, O., Ayari, M., 2011. Cultural impact in listeners' structural understanding of a Tunisian traditional modal improvisation, studied with the help of computational models. *J. Interdiscip. Music Stud.* 5, 85–100.
- Lerdahl, F., Jackendoff, R., 1983. A generative theory of tonal music. MA: MIT Press., Cambridge. MA: MIT Press.
- Lingnau, A., Downing, P.E., 2015. The lateral occipitotemporal cortex in action. *Trends Cogn. Sci.* 19,

268–277.

- Loui, P., 2015. A Dual-Stream Neuroanatomy of Singing. *Music Percept.* 32, 232–241.
- Loui, P., Li, H.C., Schlaug, G., 2011. White matter integrity in right hemisphere predicts pitch-related grammar learning. *Neuroimage* 55, 500–507.
- Loui, P., Wu, E.H., Wessel, D.L., Knight, R.T., 2009. A generalized mechanism for perception of pitch patterns. *J. Neurosci.* 29, 454–459.
- Maess, B., Koelsch, S., Gunter, T.C., Friederici, A.D., 2001. Musical syntax is processed in Broca's area : an MEG study. *Nat. Neurosci.* 4, 540–545.
- Maidhof, C., Vavatzanidis, N., Prinz, W., Rieger, M., Koelsch, S., 2009. Processing Expectancy Violations during Music Performance and Perception : An ERP Study. *J. Cogn. Neurosci.* 22, 2401–2413.
- Makuuchi, M., Bahlmann, J., Friederici, A.D., 2012. An approach to separating the levels of hierarchical structure building in language and mathematics. *Philos. Trans. R. Soc. Lond. B. Biol. Sci.* 367, 2033–2045.
- Martin, J. a., Karnath, H.-O., Himmelbach, M., 2015. Revisiting the cortical system for peripheral reaching at the parieto-occipital junction. *Cortex* 64, 363–379.
- McKiernan, K. a, Kaufman, J.N., Kucera-Thompson, J., Binder, J.R., 2003. A parametric manipulation of factors affecting task-induced deactivation in functional neuroimaging. *J. Cogn. Neurosci.* 15, 394–408.
- Musso, M., Weiller, C., Horn, A., Glauche, V., Umarova, R., Hennig, J., Schneider, A., Rijntjes, M., 2015. A Single Dual-Stream Framework for Syntactic Computations in Music and Language. *Neuroimage* 117, 267–283.
- Novembre, G., Keller, P.E., 2014. A conceptual review on action-perception coupling in the musicians' brain: what is it good for? *Front. Hum. Neurosci.* 8, 603.
- Novembre, G., Keller, P.E., 2011. A grammar of action generates predictions in skilled musicians. *Conscious. Cogn.* 20, 1232–43.
- O'Reilly, J.X., Schüfflgen, U., Cuell, S.F., Behrens, T.E.J., Mars, R.B., Rushworth, M.F.S., 2013. Dissociable effects of surprise and model update in parietal and anterior cingulate cortex. *Proc. Natl. Acad. Sci. U. S. A.* 110, E3660–9.
- Palmer, C., van de Sande, C., 1995. Range of planning in music performance. *J. Exp. Psychol. Hum. Percept. Perform.* 21, 947–62.
- Patel, A.D., 2003. Language, music, syntax and the brain. *Nat. Neurosci.* 6, 674–81.
- Pfordresher, P.Q., 2012. Musical training and the role of auditory feedback during performance. *Ann. N. Y. Acad. Sci.* 1252, 171–178.
- Power, J.D., Schlaggar, B.L., Petersen, S.E., Jonathan D. Power, Bradley L. Schlaggar, Steven E. Petersen, 2015. Recent progress and outstanding issues in motion correction in resting state fMRI. *Neuroimage* 105, 536–551.

- Rauschecker, J.P., 2011. An expanded role for the dorsal auditory pathway in sensorimotor control and integration. *Hear. Res.* 271, 16–25.
- Rauschecker, J.P., Scott, S.K., 2009. Maps and streams in the auditory cortex: nonhuman primates illuminate human speech processing. *Nat. Neurosci.* 12, 718–24.
- Rohrmeier, M. a, Koelsch, S., 2012. Predictive information processing in music cognition. A critical review. *Int. J. Psychophysiol.* 83, 164–75.
- Rohrmeier, M., Rebuschat, P., 2012. Implicit Learning and Acquisition of Music. *Top. Cogn. Sci.* 4, 525–553.
- Ruiz, M.H., Jabusch, H.-C., Altenmüller, E., 2009. Detecting wrong notes in advance: neuronal correlates of error monitoring in pianists. *Cereb. Cortex* 19, 2625–39.
- Sammler, D., Koelsch, S., Ball, T., Brandt, A., Grigutsch, M., Huppertz, H.-J., Knösche, T.R., Wellmer, J., Widman, G., Elger, C.E., Friederici, A.D., Schulze-Bonhage, A., 2013a. Co-localizing linguistic and musical syntax with intracranial EEG. *Neuroimage* 64, 134–46.
- Sammler, D., Koelsch, S., Friederici, A.D., 2011. Are left fronto-temporal brain areas a prerequisite for normal music-syntactic processing? *Cortex.* 47, 659–73.
- Sammler, D., Novembre, G., Koelsch, S., Keller, P.E., 2013b. Syntax in a pianist’s hand: ERP signatures of ‘embodied’ syntax processing in music. *Cortex.* 49, 1325–39.
- Schon, D., Anton, J.L., Roth, M., Besson, M., 2002. An fMRI study of music sight-reading. *Neuroreport* 13, 2285–2289.
- Seger, C.A., Spiering, B.J., Quraini, A.G.S.S.I., Alpeter, C., David, J., Thaut, M.H., Abstract, 2013. Corticostriatal Contributions to Musical Expectancy Perception. *J. Cogn. Neurosci.* 25:7, 1062–1077.
- Smith, S.M., Fox, P.T., Miller, K.L., Glahn, D.C., Fox, P.M., Mackay, C.E., Filippini, N., Watkins, K.E., Toro, R., Laird, A.R., Beckmann, C.F., 2009. Correspondence of the brain ’ s functional architecture during activation and rest. *PNAS* 106, 13040–13045.
- Swain, J.P., 1995. The concept of musical syntax. *Music. Q.* 79, 281–308.
- Tenenbaum, J.B., Kemp, C., Griffiths, T.L., Goodman, N.D., 2011. How to grow a mind: statistics, structure, and abstraction. *Science* 331, 1279–85.
- Tillmann, B., 2012. Music and Language Perception: Expectations, Structural Integration, and Cognitive Sequencing. *Top. Cogn. Sci.* 4, 568–584.
- Tillmann, B., Bharucha, J.J., Bigand, E., 2000. Implicit learning of tonality: {A} self-organizing approach. *Psychol. Rev.* 107, 885–913.
- Tillmann, B., Koelsch, S., Escoffier, N., Bigand, E., Lalitte, P., Friederici, a D., von Cramon, D.Y., 2006. Cognitive priming in sung and instrumental music: activation of inferior frontal cortex. *Neuroimage* 31, 1771–82.
- Tymoczko, D., 2003. Function theories: A statistical approach. *Musurgia* 10, 35–64.
- Uddin, L.Q., Kelly, A.M.C., Biswal, B.B., Castellanos, F.X., Milham, M.P., 2009. Functional

Connectivity of Default Mode Network Components: Correlation, Anticorrelation, and Causality. *Hum. Brain Mapp.* 30, 625–637.

van der Steen, M.C., Molendijk, E.B.D., Altenmueller, E., Furuya, S., 2014. Expert pianists do not listen: The expertise-dependent influence of temporal perturbation on the production of sequential movements. *Neuroscience* 269, 290–298.

Vuust, P., Witek, M. a. G., 2014. Rhythmic complexity and predictive coding: a novel approach to modeling rhythm and meter perception in music. *Front. Psychol.* 5, 1–14.

Wolpert, D.M., Flanagan, J.R., 2001. Motor prediction. *Curr. Biol.* 11, R729–R732.

Zarate, J.M., 2013. The neural control of singing. *Front. Hum. Neurosci.* 7, 237.

Zatorre, R.J., Chen, J.L., Penhune, V.B., 2007. When the brain plays music: auditory-motor interactions in music perception and production. *Nat. Rev. Neurosci.* 8, 547–58.

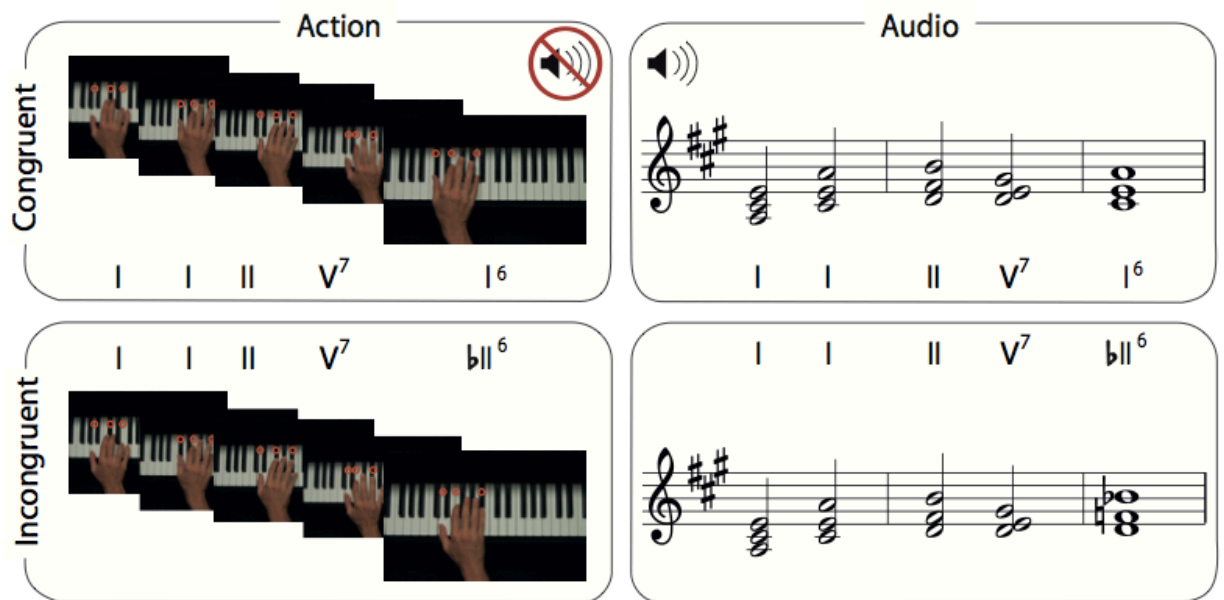


Figure 1. Experimental design: expert pianists were presented with harmonic congruent or incongruent chord progressions, presented either as muted musical actions (photos of a hand playing chords) that they were required to imitate on a glass-board (left panel), or in an auditory format that they listened to (right panel).

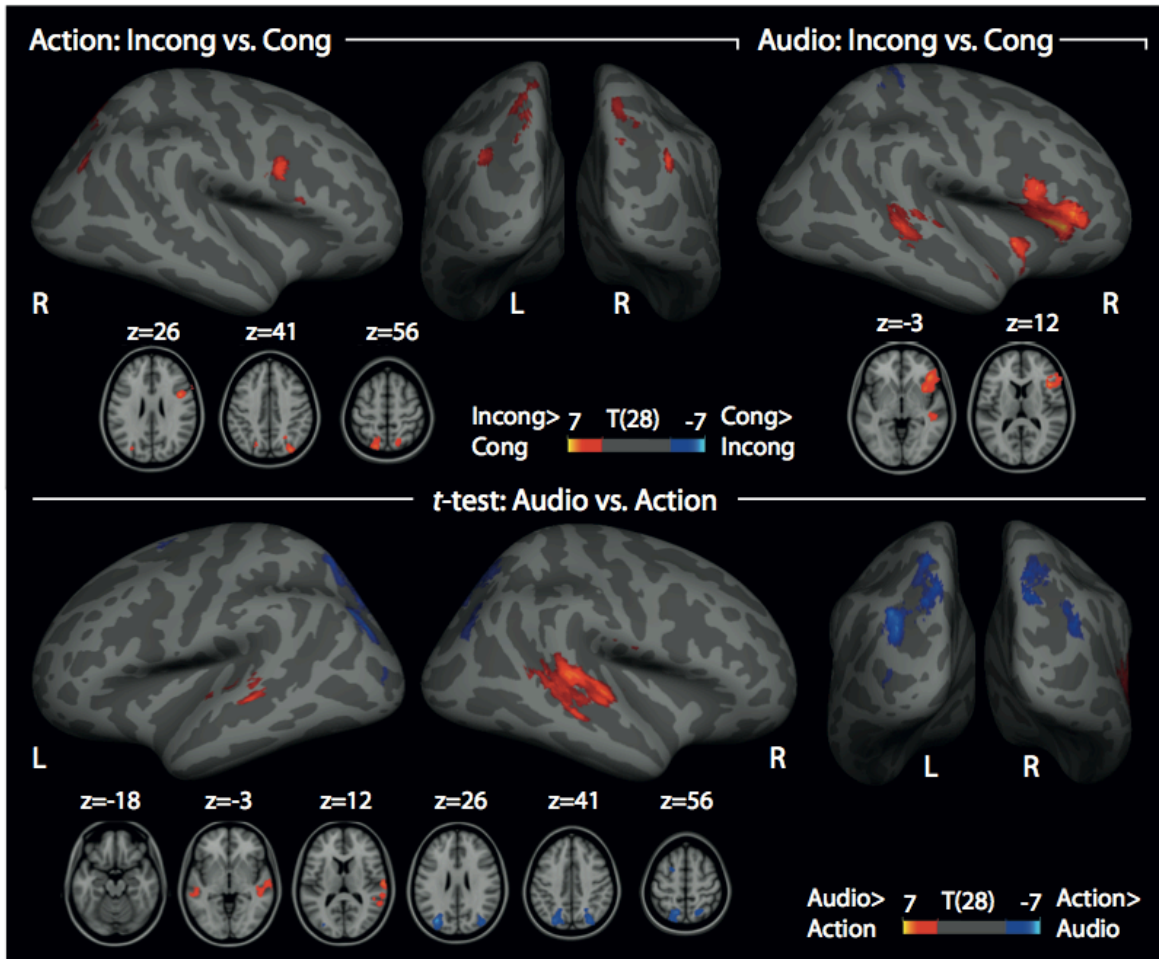


Figure 2. Harmonic violations elicited activations in fronto-parietal areas during action imitation (upper left panel) and in fronto-temporal areas during listening (upper right panel). Areas involved in structural processing specifically for the action and the audio sequences were identified in bilateral posterior parietal regions (cold colours) and in bilateral temporal regions (hot colours), respectively (lower panel).

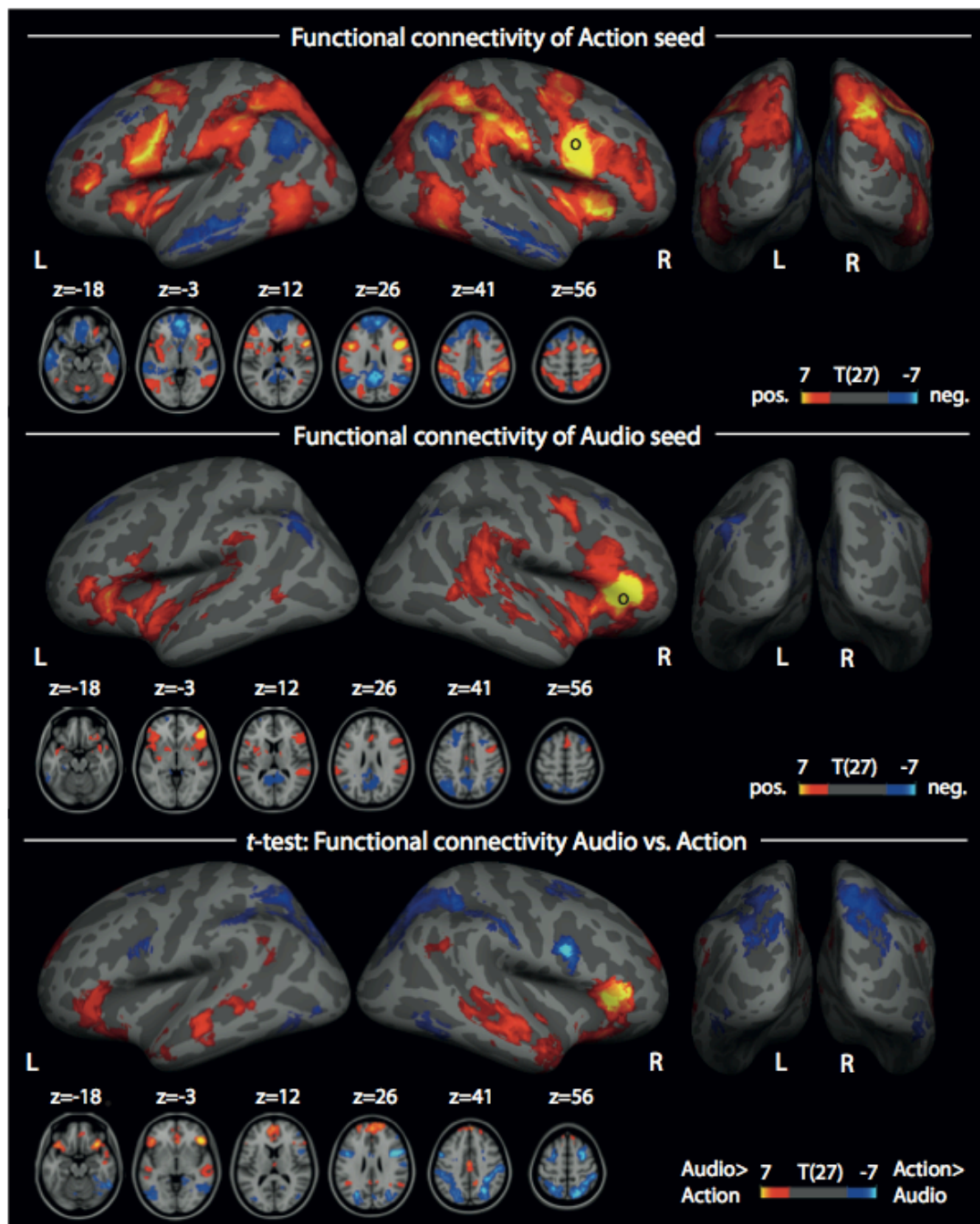


Figure 3. *Upper and middle panels:* seed-based functional connectivity maps of resting-state data from the action seed in dorsal BA44 and audio seed in BA45, respectively. Seeds are depicted as black circles. Hot and cold colours indicate positive and negative functional connectivity, respectively. Consistent with the task-based activations, the topographical connectivity patterns include posterior parietal regions from the action-seed and temporal regions from the audio-seed. *Lower panel:* *t*-test between the connectivity maps of the action- and audio seed. Correlation values in posterior parietal areas were significantly higher for the action-seed than the audio-seed, whereas temporal regions were more strongly correlated to the audio- than the action-seed.